第 49 卷 第 3 期
2022 年 3 月

湖南大学学报（自然科学版）
Journal of Hunan University (Natural Sciences)

Vol. 49 No. 3.
March 2022

Open Access Article https://doi.org/10.55463/issn.1674-2974.49.3.20

Dissimilar Joining by Ultrasonic Welding

Márton Schramkó[1,2], Zoltán Nyikes[3], Hassanen Jaber[2,4], Tünde Anna Kovács[1,*]

[1] Bánki Donát Faculty of Mechanical and Safety Engineering, Óbuda University, Budapest, Hungary

[2] Doctoral School on Materials Sciences and Technologies, Óbuda University, Budapest, Hungary

[3] Milton Friedman University, Budapest, Hungary

[4] Biomedical Engineering Department, College of Engineering, University of Thi-Qar, Nasiriyah, Iraq

Abstract: Ultrasonic welding is a rapid process for thin sheet joining. The authors wanted to show the aluminum-copper dissimilar joining by the ultrasonic welding process in this work. Ultrasonic welding is a suitable and straightforward process to establish dissimilar joints between different metals. The goal was to investigate the ultrasonic welding complex effect on the material properties. Ultrasonic welding is solid-state welding, which uses pressure, friction, ultrasound effect to establish a metallic joint. The complex effects are the friction heat, the pressure caused plastic deformation, and the ultrasound caused softening and hardening. The welding process used three kinds of geometry were, with 5 mm, 10 mm, 15 mm wide, and 80 mm length test samples. The welding is made by an ultrasonic welder machine (Branson Ultraweld L20 Spot Welder). The used parameters were the same, and the ultrasound frequency was 20 kHz. The welded spot area depended on the test sample size and the anvil sizes (12 mm x 14 mm). A microhardness tester tested the joint and the hardness of the heat-affected zone (HAZ). The hardness after the welding process showed a difference from the original hardness value of the metals. The measured results tendency is according to the literature. The ultrasound effect can cause crack propagation in the welded sheet. It was detected based on the tests that the hardness in the joint and the heat-affected zone shows differences as a function of the test sample sizes. Also detected that the crack inclination is stronger in the case of the wider sheets whiles having a bigger welded spot area. Based on the research result, it can conclude that the ultrasonically welded aluminum sheet's mechanical properties depend on the welding parameters and the welded material geometry. The results are in harmony with ultrasound softening and hardening effects theories.

Keywords: dissimilar welding, ultrasonic welding, heat-affected zone, HAZ, microhardness.

超声波焊接异种连接

摘要: 超声波焊接是一种用于薄板连接的快速工艺。作者想在这项工作中展示通过超声波焊接工艺进行的铝-铜异种连接。超声波焊接是在不同金属之间建立异种接头的合适且直接的工艺。目的是研究超声波焊接复合物对材料性能的影响。超声波焊接是固态焊接，它利用压力、摩擦、超声波效应建立金属接头。复杂的影响是摩擦热、压力引起的塑性变形以及超声波引起的软化和硬化。焊接工艺采用了三种几何形状，分别为 5 毫米、10 毫米、15 毫米宽和 80 毫米长的测试样品。焊接由超声波焊接机（必能信超焊 L20 点焊机）完成。所用参数相同

Received: 06 December, 2021 / Revised: 25 January, 2022 / Accepted: 06 February, 2022 / Published: 28 March, 2022

About the authors: Márton Schramkó, Bánki Donát Faculty of Mechanical and Safety Engineering, Óbuda University, Budapest, Hungary; Doctoral School on Materials Sciences and Technologies, Óbuda University, Budapest, Hungary; Zoltán Nyikes, Milton Friedman University, Budapest, Hungary; Hassanen Jaber2,4, Doctoral School on Materials Sciences and Technologies, Óbuda University, Budapest, Hungary; Biomedical Engineering Department, College of Engineering, University of Thi-Qar, Nasiriyah, Iraq; Tünde Anna Kovács1, Bánki Donát Faculty of Mechanical and Safety Engineering, Óbuda University, Budapest, Hungary

Corresponding author Tunde Anna Kovacs, kovacs.tunde@uni-obuda.hu

，超声频率为 20 千赫。焊点面积取决于测试样品尺寸和砧座尺寸 (12 毫米 x 14 毫米)。显微硬度计测试接头和热影响区的硬度。焊接后的硬度与金属的原始硬度值有差异。测量结果趋势与文献一致。超声波效应会导致焊接板中的裂纹扩展。根据测试检测到，接头和热影响区的硬度显示出作为测试样本大小的函数的差异。还检测到，在具有较大焊点面积的情况下，较宽的板材裂纹倾向更强。根据研究结果，可以得出结论，超声波焊接铝板的力学性能取决于焊接参数和焊接材料的几何形状。结果与超声软化和硬化效应理论一致。

关键词：异种焊接, 超声波焊接, 热影响区, 热影响区, 显微硬度。

1. Introduction

Ultrasonic welding nowadays is a standard process in industrial applications. Ultrasonic welding is helpful for microelectronic application manufacturing because of the low temperature and suitable joint strengths [1]. Ultrasonic welding is a solid-state process that is very rapid and environmentally friendly. The joining in the case of different metals is also possible through the ultrasonic welding process. During ultrasonic welding, it can detect several effects, like plastic deformation, friction heat, and ultrasound effects. The theoretical background of ultrasonic welding is usually the plastic deformation of the metals and the acoustoplasticity, also known as the Blaha effect or ultrasonic softening [1-3]. The ultrasonic effect can cause the modification of the microstructure and the dislocation density [2]. The critical effect of the process is ultrasonic softening, which helps to establish a bond with plastic deformation. The welding process uses friction, which initiates low heating in the bond. The heat generation depends on several parameters, but it was detected that the established friction heat could earn 250 °C [4]. The technology's physical base is the electroacoustic and plastic deformation effect, assisted by the heat established from the friction-affected plastic deformation in the metal crystal structure. The high-frequency vibration of the ultrasound transmits energy to the crystal structure [5]. Ultrasonic welding unit several effects like high-frequency vibration, pressure caused plastic deformation, and the vibration amplitude limited friction. These effects establish a metallic joint between the metal sheets. The ultrasonic welding process modifies the crystal structure as a function of the technological properties depending on the lattice parameters and defects. The material plasticity and mechanical properties of the materials are based on the dislocation theory is well introduced and highlighted in several scientifical articles. The plastic deformation theories in the case of the FCC crystal structure materials are known [5-7]. The technical materials event the metals have many defects in their crystal structure. Taylor and independently the Orowan and Polányi theories for the phenomena of the plastic deformation were the pioners applied concepts of the dislocation theory. Dislocations are not stable formations the density of the dislocation depends on several parameters [8]. The thermal condition and the cold working caused work-hardening can modify the dislocation density. The ultrasonic process parameters optimization needs to know the metal properties [8, 9]. The optimization can be complicated in dissimilar welding processes.

The joining of aluminum and copper thin sheets or cables is an industrial request for electronic applications and batteries. In these applications, the high-temperature welding (fusion welding) processes are not suitable to establish dissimilar joints, as electronic devices can be damaged by heat shock. During dissimilar welding, it needs to consider a minimum of two different materials. These materials have different thermal, mechanical properties based on their chemical composition and crystal structure.

Ultrasonic welding is complex effects united solid-state process that can be understood based on the physical and crystallography knowledge like plasticity and vibration transmitted energy effects [10-14]. The reason for the established joint mechanical and microstructural properties is notable by the results of material science [15-17]. This work aims to find a relationship between the technologies parameters, the workpiece geometry, and the established joint mechanical properties.

2. Materials and Methods

2.1. Materials

A pure half hard aluminum sheet (EN AW-1050A, H14/H24, WrN. 3.0255) and a pure rolled copper sheet (EN Cu-DHP/CW024A, DIN- WrN. 2.0090).

Table 1 shows the chemical composition of the used metals. The aluminum test sample's measured hardness (Zwick 3212 microhardness tester) was 33.63 $HV_{0.2}$, and the hardness of the copper was 74.43$HV_{0.2}$. The thickness of both sheets was 0,5 mm.

Table 1 Three-line representation

Element of EN AW-1050A (w/w%)							
Fe	Si	Cu	Mn	Zn	Ti	Al	Other
0.4	0.25	0.05	0.05	0.07	0.05	99.98	0.03
Element of EN Cu-DHP/CW024A (w/w%)							
Cu	P						Other
99.9	0.25						0.075

For the welding test, it was used rectangular test samples were with different wideness; it is shown in Fig. 1.

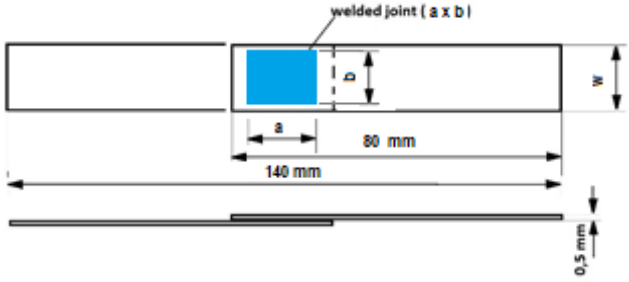

Fig. 1 Test sample geometry

The sizes of the test samples are collected in Table 2.

Table 2 Test samples sizes (following Fig. 1.)

ID	w (mm)	a (mm)	b (mm)	axb (mm^2)
N3	15	14.5	14.5	210.25
N2	10	14.5	10	145
N1	5	14.5	5	72.5

2.2. Ultrasonic Welding

The ultrasonic welding process was carried out with the Branson Ultraweld L20 welder machine (Fig. 2). The used frequency was 20 kHz. The applicable pre-pressure (TP) and welding pressure (WP) are between 10-80 Psi; maximal Power is 4 kW. For the welding process, we determined the following welding parameters; welding time t (s), amplitude A (µm), maximum 60 µm pre-pressure TP (Psi), welding pressure WP (Psi). The used welding parameters are shown in Table 3.

Table 3 Used welding parameters

Welding parameters	Value
welding time t (s)	0.7
amplitude A (µm)	42
pre-pressure TP (Psi)	15
welding pressure WP (Psi)	15

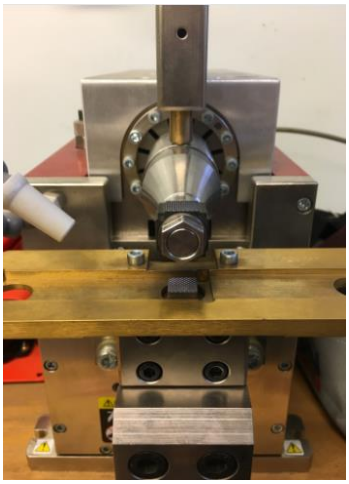

Fig. 2 Branson Ultraweld L20 instrument (Branson Ultrasonics Corporation USA)

It was used the same parameters in the case of all welding tests. The welded joints are shown in Fig. 3. In the case of the 15 mm wide test sample (Test sample number 3), the aluminum side of the dissimilar joint seems to have plastic deformation in the heat-affected zone (HAZ).

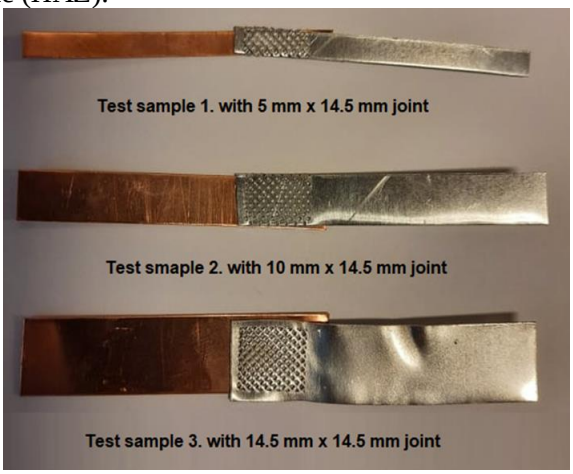

Fig. 3 The welded test samples

The HAZ determination is not the best expression for this area because the temperature in this part is lower than the recrystallization temperature (as we concede the recrystallization temperature like the bordering temperature of the HAZ). Nevertheless, it can determine some heating. Also, it can determine in this area some mechanical properties modification.

2.3. Materials Characterization

Samples for metallographic examination through the cross-section were prepared using the standard metallography procedure and etched by ammonium persulfate ($(NH_4)2S_2O_8$). The cross-section of the dissimilar Al-Cu joint was visually tested using a Neophot 2 Optical Microscope (Jena, Germany, Carl Zeiss) after etching.

2.4. Hardness Test

The microhardness tests were achieved by Zwick

3212 microhardness tester; the used load was 0.2 kg and standard Vickers diamond indenter. The hardness was determined in the center point of the joint and the HAZ (10, 20, 30 mm from the center point) on dissimilar joints' sides.

2.5. Transmission Electron Microscopy (TEM)

The TEM investigation was carried out by TEM-JEOL, Model- JEM 2100F, Specification- Resolution: Point: 0.19 nm Line: 0.1. TEM images are formed using transmitted electrons (instead of the visible light) which can produce magnification details up to 50 x - 1.5M x with accelerating Potential: 200 kV Attachment Systems: EDS, STEM. The images can be resolved over a fluorescent screen. Furthermore, the X-ray analysis produced by the interaction between the accelerated electrons with the sample allows for determining the sample's elemental composition with high spatial resolution.

The following processes made TEM samples prepared:

• Samples cutting:- One piece of Al or Cu substrate size 3 x 3mm small disc is cut with the help of a holder an ultrasonic cutter. The tool's shape is circular to produce a disk 3 mm in diameter. Substrate parallel to the cutting tool, a spring-loaded platform helps to apply a constant force by pressing the sample up against the samples.

• Mechanical grinding:- After cutting out 3mm discs, mechanical polishing is used to thin the substrate and produce smooth, scratch-free surfaces before dimpling. Samples rotate in a circular direction on wet diamond paper using a disc grinder with large grit size 500, 1200, 2400, and 4000. The samples must be checked under an optical microscope to determine scratches or defects.

• Punch grinding machine:- After mechanical grinding, substrates are kept in the front of the punching machine, and the grinding disc is parallelized so that the grinding process can be performed in the center part. First, open the pressing handle and place the punch between the rotating roller and the pressure bearing. The screws with the pressing handle adjust the pressure bearing so that the pressure bearing can touch the center of the punch on the substrate. Due to the pressure of the punch being slightly depressed then, the direction of the substrate keeps rotating 60-100 times in 1min. During the rotation, the sharpening stone touches the punch and gradually grinds.

• Dimpling/Polishing:-After maintaining 80µm thin samples, one side part is only dimpled with a 15 mm diameter SS wheel for the grinding stage using oil-based diamond paste. Polishing occurs in 2 stages with a soft felt wheel: extra grind-ing/polishing using 1 and 0.25 µm oil-based diamond paste as long as required, followed by a short polishing stage using 0.05 µm alumina suspension. With the application of the same soft felt wheel, the flat side is polished only using a sequence of 1 µm diamond paste for 120 s, 0.25 m to 60 s, finalized by polishing with an alumina suspension for 2 min.

• Final prepared all substrate ~20µm should be carefully deposited on a 3 mm carbon-coated commercially available copper grid. Then grid could be fixed on the TEM sample holder for characterization.

3. Results and Discussion

3.1. Microscopy of the Joint Cross-Section

The microscopy picture is shown in Fig. 4, which shows that the typical solid-state welded joint evolved. The joint wave follows the clamping anvil surface geometry. Therefore, it cannot detect any inclusion, imperfection, or crack.

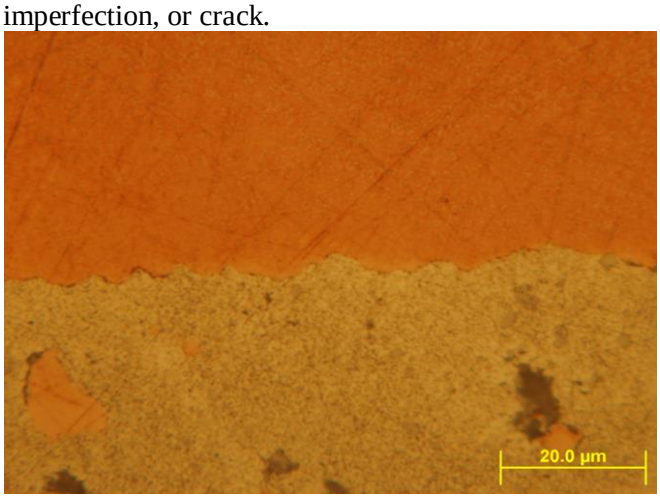

Fig. 4 The welded test samples

3.2. Hardness Test Results

We made a hardness test to determine the ultrasonic welding effects in the welded joint and the HAZ. Also, we wanted to determine the effect of the joint area. Because we observed that the process results depend on the test sample sizes. The ultrasonic softening wanted also verified. The hardness test results are assembled in Table 4. The hardness of the welded samples is different from the original material hardness. (The aluminum test sample was 33.63 $HV_{0.2,}$ and the hardness of the copper was 74.43$HV_{0.2}$.).

Table 4 Hardness results

ID	Hardness $HV_{0.2}$			
distance	0 mm	10 mm	20 mm	30 mm
N3 Al	25.12	24.48	23.2	20.91
N3 Cu	106.52	76.4	72.03	68.02
N2 Al	59.92	40.1	40.44	31.4
N2 Cu	78.64	80.58	74.96	76.4
N1 Al	60	37.83	37.08	40.23
N1 Cu	103.57	80.19	83.43	74.6

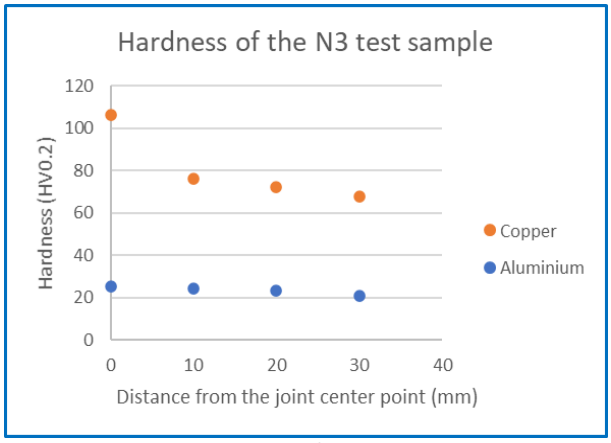

Fig. 5 The hardness of the test sample N3

The hardness of the test sample N3 decreased due to the distance from the joint center point (Fig. 5). The hardness of the dissimilar joint on the aluminum side was lower than the original hardness of the aluminum sheet. The copper side of the joint showed higher hardness than the original one.

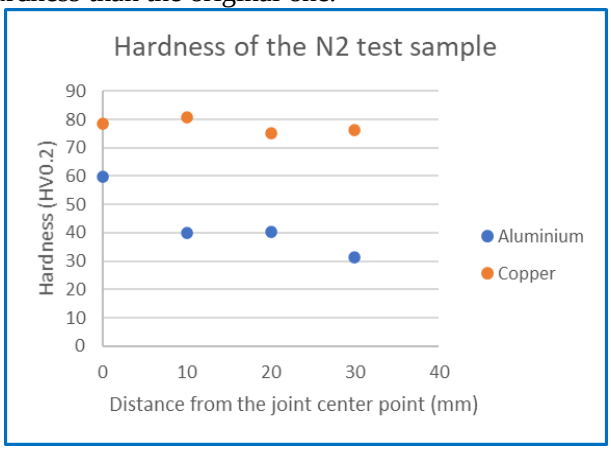

Fig. 6 The hardness of the test sample N2

The hardness of the test sample N2 decreased due to the distance from the joint center point (Fig. 6.). The hardness of the dissimilar joint on the aluminum side increased. The copper side of the joint showed higher hardness than the original one.

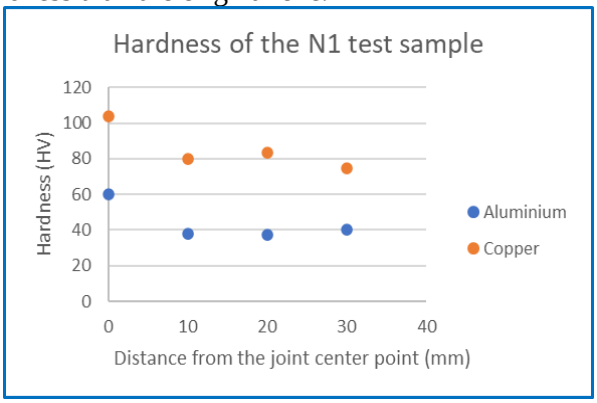

Fig. 7. The hardness of the test sample N1

The hardness of the test sample N2 decreased due to the distance from the joint center point (Fig. 7). The hardness of the dissimilar joint on both sides hardened, and the hardness decreased was different than in the case of the N2and N3 test samples.

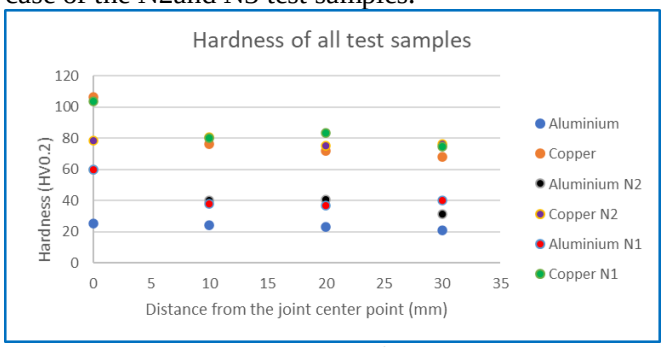

Fig. 8. The hardness of all test samples

Fig. 8 shows the tendency as a function of the joint distance the hardness.

3.3. TEM

The TEM results show the dislocations after the ultrasonic welding. It can compare the HAZ structure of the welded metals. The TEM test was made on test sample N3.

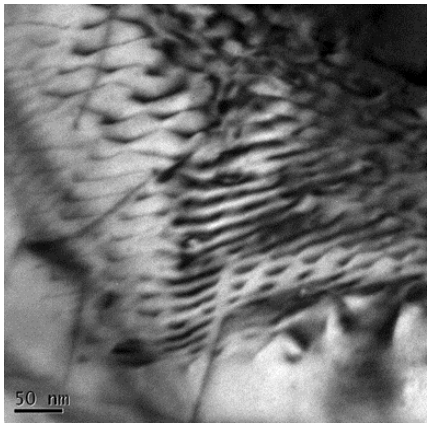

Fig. 9. N3 sample HAZ of the aluminum side (10 mm from the joint center point)

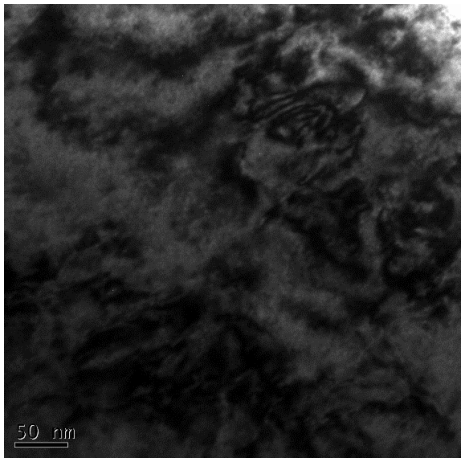

Fig. 10. N3 sample HAZ of the copper side(10 mm from the joint center point)

The TEM results show different dislocation forms in the aluminum and the copper HAZ. The dislocation density is higher than in the case of the unwelded metals. The plastic deformation [6] and the ultrasound effect [2] increase dislocation density. The investigation results are in harmony with the literature

[2, 6].

4. Conclusion

Based on the investigation results, it can conclude that the complex ultrasonic effects modified the mechanical properties of the welded metal.

1. The microscopy evaluation showed that the ultrasonic welding parameters are suitable for establishing a joint between the half-hard aluminum sheet (EN AW-1050A, H14/H24, WrN. 3.0255) and a pure rolled copper sheet (En Cu-DHP/CW024A, DIN-WrN. 2.0090). The established joint straightness in the case of the optimal welding parameters was higher than the base metal.
2. The hardness test results showed that in the HAZ, the hardness is lower than in the welded joint. The reason for the softening in the HAZ can be the ultrasound softening effect. The heating caused by friction is lower than the recrystallization temperature cannot be the reason for the softening.
3. The hardness is smaller than the used original aluminum sheet hardness in the case of the most significant spot area and more significant in the case of the smaller spot area under the same welding process parameters. These results are explicable by the complex effect of ultrasonic welding. The heating from the friction and the ultrasound softening effects are higher in the case of the higher surface area.
4. The hardening effect reason is not defined; it needs more tests to understand this effect. Although, ultrasound softening and hardening effect depends on the contact area. The earned hardness results confirm the theory.
5. Probable that the joint hardness depends on the spot area size. The experimental results are in harmony with the theoretical background. The ultrasonic welding complex effects, the used test sample geometry, and the metal's basic mechanical properties collectively result in the joint and HAZ mechanical properties. Therefore, it can conclude that the used parameters in the used welding instrument are suitable for industrial applications.

References

[1] SIDDIQ A., & GHASSEMIEH E. Thermomechanical analyses of ultrasonic welding process using thermal and acoustic softening effects. *Mechanics of Materials*, 2008, 40: 982-1000. https://doi.org/10.1016/j.mechmat.2008.06.004

[2] LANGENECKER B. Effects of Ultrasound on Deformation Characteristics of Metals. *IEEE Transactions on Sonics and Ultra-sonics*, 1966, 13(1): 1–8. https://doi.org/10.1109/t-su.1966.29367

[3] ZHOU H., CUI H., and QIN Q. Influence of ultrasonic vibration on the plasticity of metals during compression process. *Journal of Materials Processing Technology*, 2018, 251: 146-159. https://doi.org/10.1016/j.jmatprotec.2017.08.021

[4] BHUDOLIA S. K., GOHEL G., LEONG K. F., and ISLAM A. Advances in Ultrasonic Welding of Thermoplastic Composites: A Review. *Materials*, 2020, 13(6): 1284. https://doi.org/10.3390/ma13061284

[5] WARD A. A., FRENCH M. R., LEONARD D. N., and CORDERO Z. C. Grain Growth During Ultrasonic Welding of Nanocrystalline Alloys. *Journal of Materials Processing Technology*, 2018, 254: 373-382. https://doi.org/10.1016/j.jmatprotec.2017.11.049

[6] KOVÁCS I., & ZSOLDOS L. *Dislocations and Plastic Deformation*. Pergamon Press Ltd., Oxford, 1973.

[7] DESHPANDE A., TOFANGCHI A., and HSU K. Microstructure evolution of Al6061 and copper during ultrasonic energy-assisted compression. *Materials Characterization*, 2019, 153: 240-250. https://doi.org/10.1016/j.matchar.2019.05.005

[8] DHARA S., & DAS A. Impact of ultrasonic welding on multi-layered Al-Cu joint for electric vehicle battery applications: A layer-wise microstructural analysis. *Materials Science and Engineering*, 2020, 139795: 1-47. https://doi.org/10.1016/j.msea.2020.139795

[9] FUJII H. T., ENDO H., SATO Y. S., and KOKAWA H. Interfacial microstructure evolution and weld formation during ultrasonic welding of Al alloy to Cu. *Materials Characterization*, 2018, 139, 233–240. https://doi.org/doi:10.1016/j.matchar.2018.03.010

[10] SEDAGHAT H., ZHANG W., and XU L. Ultrasonic Vibration-Assisted Metal Forming: Constitutive Modelling of Acoustoplasticity and Applications, *Journal of Materials Processing Technology*, 2018, 15965: 1-35. https://doi.org/10.1016/j.jmatprotec.2018.10.012

[11] PENG H., CHEN D., and JIANG X. Microstructure and Mechanical Properties of an Ultrasonic Spot Welded Aluminum Alloy: The Effect of Welding Energy, *Materials*, 2017, 10, 449, 1-16. https://doi.org/10.3390/ma10050449

[12] RUSINKO A. Modeling the Effect of DC on the Creep of Metals in Terms of the Synthetic Theory of Irrecoverable Deformation. *Mechanics of Materials*, 2016, 93: 163-167. https://doi.org/10.1016/j.mechmat.2015.10.016

[13] KITAEVA D. A., RUDAEV Y. I., RUDSKOY A. I., and KODZHASPIROV G. E. On Dynamic Superplasticity of Aluminum Alloys with Initial Varying Grain Size Structure. *Defect and Diffusion Forum*, 2018, 38: 78–83. https://doi.org/10.4028/www.scientific.net/DDF.385.78

[14] RUSZINKÓ E., & ALHILF A. H. The Effect of Ultrasound on Strain-hardened Metals. *Acta Polytechnica Hungarica*, 2021, 18(8): 221-233. http://acta.uni-obuda.hu/Ruszinko_Alhilfi_115.pdf

[15] CHINH N. Q., & KOVÁCS Z. S. Unique microstructural and mechanical properties of Al-Zn alloys processed by high-pressure torsion. *IOP Conf. Series: Materials Science and Engineering*, 2019, 613(012028): 1-6. https://doi.org/10.1088/1757-899X/613/1/012028

[16] BURŠÍK J., BURŠÍKOVÁ V., ROGL G., and ROGL P. Local mechanical properties of advanced skutterudites processed by various routes. *IOP Conference Series: Materials Science and Engineering*, 2019, 613(012036): 1-4. https://doi.org/10.1088/1757-899X/613/1/012036

[17] YANG J., CAO B., and LU Q. The Effect of Welding Energy on the Microstructural and Mechanical Properties of Ultrasonic-Welded Copper Joints. *Materials*, 2017, 10(193): 1-13. https://doi.org/10.3390/ma10020193

参考文:

[1] SIDDIQ A., 和 GHASSEMIEH E. 使用热和声软化效应对超声波焊接过程进行热机械分析。**材料力学**, 2008, 40: 982-1000. https://doi.org/10.1016/j.mechmat.2008.06.004

[2] LANGENECKER B. 超声波对金属变形特性的影响。电气和电子工程师学会声波和超声波交易, 1966, 13(1): 1–8. https://doi.org/10.1109/t-su.1966.29367

[3] ZHOU H., CUI H., 和 QIN Q. 超声振动对压缩过程中金属塑性的影响[J].**材料加工技**术学报, 2018, 251: 146-159. https://doi.org/10.1016/j.jmatprotec.2017.08.021

[4] BHUDOLIA S. K., GOHEL G., LEONG K. F., 和 ISLAM A. 热塑性复合材料超声焊接的进展：综述。**材料**, 2020, 13(6): 1284. https://doi.org/10.3390/ma13061284

[5] WARD A. A., FRENCH M. R., LEONARD D. N., 和 CORDERO Z. C. 纳米晶合金超声焊接过程中的晶粒生长。**材料加工技**术学报, 2018, 254: 373-382. https://doi.org/10.1016/j.jmatprotec.2017.11.049

[6] KOVÁCS I., 和 ZSOLDOS L. 位错和塑性变形。**佩加蒙出版社有限公司，牛津**, 1973.

[7] DESHPANDE A., TOFANGCHI A., 和 HSU K. 超声能量辅助压缩过程中 Al6061 和铜的微观结构演变。**材料表征**, 2019, 153: 240-250. https://doi.org/10.1016/j.matchar.2019.05.005

[8] DHARA S., 和 DAS A. 超声波焊接对电动汽车电池应用多层铝铜接头的影响：分层微观结构分析。**材料科学与工程**, 2020, 139795: 1-47. https://doi.org/10.1016/j.msea.2020.139795

[9] FUJII H. T., ENDO H., SATO Y. S., 和 KOKAWA H. 铝合金与铜超声焊接过程中的界面组织演变和焊缝形成。**材料表征**, 2018, 139, 233–240. https://doi.org/doi:10.1016/j.matchar.2018.03.010

[10] SEDAGHAT H., ZHANG W., 和 XU L. 超声波振动辅助金属成形：声塑性和应用的本构建模，**材料加工技**术杂志, 2018, 15965: 1-35. https://doi.org/10.1016/j.jmatprotec.2018.10.012

[11] PENG H., CHEN D., 和 JIANG X. 超声波点焊铝合金的显微组织和力学性能：焊接能量、**材料的影响**, 2017, 10, 449, 1-16. https://doi.org/10.3390/ma10050449

[12] RUSINKO A. 根据不可恢复变形的综合理论模拟 DC 对金属蠕变的影响。**材料力学**, 2016, 93: 163-167. https://doi.org/10.1016/j.mechmat.2015.10.016

[13] KITAEVA D. A., RUDAEV Y. I., RUDSKOY A. I., 和 KODZHASPIROV G. E. 初变晶粒结构铝合金的动态超塑性研究。**缺陷与**扩散论坛, 2018, 38: 78–83. https://doi.org/10.4028/www.scientific.net/DDF.385.78

[14] RUSZINKÓ E., 和 ALHILF A. H. 超声波对应变硬化金属的影响。**匈牙利理工学院学**报, 2021, 18(8): 221-233. http://acta.uni-obuda.hu/Ruszinko_Alhilfi_115.pdf

[15] CHINH N. Q., 和 KOVÁCS Z. S. 高压扭转加工的铝锌合金独特的显微组织和力学性能。**物理研究所系列**：**材料科学与工程**, 2019, 613(012028): 1-6. https://doi.org/10.1088/1757-899X/613/1/012028

[16] BURŠÍK J., BURŠÍKOVÁ V., ROGL G., 和 ROGL P. 各种途径加工的高级方钴矿的局部力学性能。**物理研究所系列会**议：**材料科学与工程**, 2019, 613(012036): 1-4. https://doi.org/10.1088/1757-899X/613/1/012036

[17] YANG J., CAO B., 和 LU Q. 焊接能量对超声波焊接铜接头微观结构和力学性能的影响。**材料**, 2017, 10(193): 1-13. https://doi.org/10.3390/ma10020193